PHYSICAL REVIEW D **89,** 053013 (2014)

Radiative emission of neutrino pair from nucleus and inner core electrons in heavy atoms

M. Yoshimura[1] and N. Sasao[2]

[1]*Center of Quantum Universe, Faculty of Science, Okayama University, Tsushima-naka 3-1-1 Kita-ku, Okayama 700-8530, Japan*

[2]*Research Core for Extreme Quantum World, Okayama University, Tsushima-naka 3-1-1 Kita-ku, Okayama 700-8530, Japan*

(Received 30 October 2013; published 25 March 2014)

Radiative emission of neutrino pair from atomic states is a new tool to experimentally investigate undetermined neutrino parameters such as the smallest neutrino mass, the nature of neutrino masses (Majorana vs Dirac), and their *CP* properties. We study effects of neutrino pair emission either from inner core electrons or from the nucleus in which the zeroth component of quark or electron vector current gives rise to large coupling. Both the overall rate and the spectral shape of photon energy are given for a few cases of interesting target atoms. Calculated rates exceed those of previously considered target atoms by many orders of magnitude.

DOI: 10.1103/PhysRevD.89.053013 PACS numbers: 14.60.Pq, 14.60.Lm

I. INTRODUCTION

Recent developments of neutrino oscillation experiments have achieved remarkable success: Many elements of the fundamental neutrino mass matrix have been determined, including all three mixing angles and two mass squared differences [1]. However, they left undetermined the absolute scale of neutrino masses (or equivalently the smallest neutrino mass), the nature of masses (Dirac or Majorana type), and their *CP* properties. Conventional targets in ongoing experiments exploring these undetermined neutrino properties and parameters have been nuclei. Direct measurement of the end point spectrum of beta decay, such as tritium [2], and (neutrinoless) double beta decay [3] are two main methods to resolve these outstanding problems.

Some time ago we proposed to use atomic transitions for improved exploration of undetermined neutrino properties [4,5]. The idea is to exploit the fact that atomic level spacings are much closer to expected neutrino masses, and many experimental methods are available to manipulate atomic transitions. The process we use is macrocoherent atomic deexcitation: $|e\rangle \to |g\rangle + \gamma + \nu_i\nu_j$ where $\nu_i, i = 1,2,3$ are neutrino mass eigenstates. By measuring the photon energy spectral shape (different from the one of spontaneous decay) one can determine locations of six thresholds at $\omega_{ij} \equiv \epsilon_{\rm eg}/2 - (m_i + m_j)^2/(2\epsilon_{\rm eg})$ ($\epsilon_{\rm eg}$ is the atomic level spacing) associated with the pair emission $\nu_i\nu_j$, and determine all neutrino masses with precision, if the macrocoherence we proposed [6] works as expected. The Majorana vs Dirac distinction is made possible due to the interference effect of identical Majorana fermions [4].

The key idea to enhance otherwise small weak rates for atomic electrons is the use of macrocoherence, which may change rates $\propto nV = N$ (the total number of target atoms) to rates $\propto n^2V$. Here n is the number density of target atoms within some unit volume of a macroscopic region such as cm^{-3}, related neither to the small atomic size nor the wavelength of emitted photon, and may be taken much larger.

A prerequisite for an experimental success is thus the development of macrocoherence, which is triggered by two laser fields accompanying target polarization [6]. Macrocoherent radiative emission of neutrino pair has been called RENP for brevity. In our preceding works neutrino pair emission from valence electrons alone has been considered, the emission vertex being M1 (magnetic dipole) type (actually the spin current). The interaction of electron with neutrino contains both charged W and neutral Z exchange diagrams, and the axial vector part of electron current contributed to this form.

Macrocoherence that gives rise to a large enhancement $\propto n^2V$ is related to the additional effect of momentum conservation in atomic process in the following way. The RENP rate of a macroscopic body of targets is obtained from the squared amplitude, $|\sum_i^N \mathcal{M}_i e^{i(\vec{k}+\vec{p}_1+\vec{p}_2)\cdot\vec{x}}|^2$ where $\vec{k}$ is the photon momentum and $\vec{p}_i$ is momenta of the emitted neutrino pair. In the spontaneous decay the phase factor in $\mathcal{M}_i$ at each atomic site i is random and, due to the large atomic mass the atomic recoil, may be neglected. Thus, in the spontaneous decay one has the continuous photon energy spectrum starting from the energy difference $\epsilon_{\rm eg}$ of atomic levels. If the phase coherence works as in the case of macrocoherent RENP, the phase factor in $\mathcal{M}_i$ is slowly varying, or is almost constant for the whole body of target atoms. One then has the enhanced rate at the point of the phase space of $\vec{k} + \vec{p}_1 + \vec{p}_2 = 0$. Thus, the momentum-conserving portion of the energy spectrum is enhanced with the factor $\propto n^2V$. This gives rise to the photon energy spectrum with stepwise increase at thresholds,

ω_{ij}, providing the advantage of resolving the neutrino mass thresholds. The spontaneous part of radiative emission of neutrino pair has a very small rate and is completely negligible compared to the macrocoherent RENP. The development of macrocoherence is achieved by the two-photon process called paired superradiance (PSR) and is described by a master equation [5] that describes both the evolving atomic polarization and trigger electromagnetic fields.

In the present work we examine new types of neutrino pair emission: emissions from core electrons and nucleus instead of valence electrons, both arising from the zeroth component of a vector current of monopole nature. The relevant monopole current counts the number of constituents, hence one may expect a large contribution from heavy atoms. A similar enhancement due to the nuclear monopole current has been used in experiments that have established atomic parity violation [7–10]. The nuclear monopole interaction that gives rise to the largest rates is not sensitive to Majorana CP phases (but is sensitive to Majorana vs Dirac distinction), while smaller rates of pair emission from valence electrons have a sensitivity to CP phases. It seems that for complete determination of the neutrino mass matrix one needs a variety of targets, presumably with different technological strategies.

We shall give the photon energy spectrum of RENP for Cs and Xe. Alkali atoms are chosen as the simplest atom to show our fundamental ideas, and Xe is interesting as it leaves room for the possibility of performing RENP experiments in the gas target. Different targets have special features of merits and demerits. Further detailed study is necessary to select the best candidate atoms.

The present work is organized as follows. In Sec. II the important idea of Coulomb-assisted RENP, which gives rise to enhancement by a high power of Z, is explained and formulated. In Sec. III, the RENP spectral rate that gives the largest rate is given and some numerical example of the spectral shape is illustrated. Finally, we summarize present work in Sec. IV. In two Appendices, we give a rudimentary account of the Thomas-Fermi model used for the estimate of Coulomb integral in heavy atoms, and we calculate the phase space integration over neutrino momenta.

II. COULOMB-ASSISTED NEUTRINO PAIR EMISSION FROM NUCLEUS AND CORE ELECTRONS

The four-Fermi interaction of neutrinos with atomic electrons and quarks in nucleus is given by

$$H_w = \langle n| \int dx^3 (\mathcal{H}^e_{2\nu}(x) + \mathcal{H}^q_{2\nu}(x))|n'\rangle, \tag{1}$$

$$\mathcal{H}^e_{2\nu} = \frac{G_F}{\sqrt{2}} \Big(\bar{\nu}_e \gamma^\alpha (1-\gamma_5)\nu_e \bar{e}\gamma_\alpha(1-\gamma_5)e - \frac{1}{2}\sum_i \bar{\nu}_i \gamma^\alpha(1-\gamma_5)\nu_i \bar{e}\gamma_\alpha(1-4\sin^2\theta_W-\gamma_5)e \Big), \tag{2}$$

$$\mathcal{H}^q_{2\nu} = \frac{G_F}{\sqrt{2}} \sum_i \bar{\nu}_i \gamma_\alpha (1-\gamma_5)\nu_i j^\alpha_q, \tag{3}$$

$$j^\alpha_q = \frac{1}{2}(\bar{u}\gamma^\alpha(1-\gamma_5)u - \bar{d}\gamma^\alpha(1-\gamma_5)d) - 2\sin^2\theta_W \left(\frac{2}{3}\bar{u}\gamma^\alpha u - \frac{1}{3}\bar{d}\gamma^\alpha d \right). \tag{4}$$

As usual, the electron neutrino ν_e is a mixture of three mass eigenstates, ν_i; $\nu_e = \sum_i U_{ei}\nu_i$. The neutrino interaction with quarks for RENP is mediated only by Z-exchange interaction.

We shall first consider neutrino interaction with atomic electrons, arising from the term $\mathcal{H}^e_{2\nu}$. Atomic electrons may be treated as nonrelativistic and this gives two main contributions: the spin three-vector $e^\dagger\vec{\sigma}e$ from the four-axial vector current and the monopole charge density $e^\dagger e$ from the four-vector current. For transitions in heavy atoms the monopole contribution from all electrons within the closed shell is expected to be large, since there are (of order) Z electrons, unlike a single or a few valence electrons. The contribution of the spin vector term $\propto \vec{\sigma}$ cancels among most of the core electrons. In what follows, we shall therefore consider as the dominant contribution the monopole weak interaction of the form written in terms of two component spinor fields,

$$\mathcal{H}^e_{2\nu} = \frac{G_F}{\sqrt{2}} e^\dagger e \sum_{ij} b_{ij}\nu^\dagger_j(1-\gamma_5)\nu_i + O\left(\frac{1}{m_e}\right), \tag{5}$$

$$b_{ij} = U_{ei}U^*_{ej} - \frac{1}{2}\delta_{ij}(1-4\sin^2\theta_W), \quad 1-4\sin^2\theta_W \sim 0.044. \tag{6}$$

We consider the neutrino pair emission from one of core electrons in a state $|c\rangle$ and dipole (E1) photon emission from an excited state $|v'\rangle$, first without the Coulomb interaction. In the nonrelativistic perturbation theory there are two ways in time sequence in which monopole core emission of vertex $b_{ij}\langle c|c\rangle = b_{ij}$ and E1 vertex $\langle v|\vec{d}\cdot\vec{E}|v'\rangle$ are arranged. When the contributions from these two diagrams are added, they give amplitudes of the form

$$b_{ij}\langle v|\vec{d}\cdot\vec{E}|v'\rangle \left(\frac{1}{\epsilon_{v'} - \epsilon_v - \omega} + \frac{1}{-E_{2\nu}} \right), \tag{7}$$

with $E_{2\nu}$ the total energy of two neutrinos. Two terms in the bracket of this equation are the usual energy denominator factor in the second order perturbation theory. The energy conservation for the process $|v'\rangle \to |v\rangle + \gamma + \nu_i\nu_j$ gives $E_{2\nu} = \epsilon_{v'} - \epsilon_v - \omega$, hence these two contributions exactly cancel.

Radiative neutrino pair emission from core electrons thus becomes effective only when it is accompanied by

Coulomb interaction between core electrons and valence electrons, which is needed to emit a photon. We shall thus consider the third order perturbation of Coulomb-assisted neutrino pair emission, which has matrix elements between two antisymmetrized wave functions of valence and core electrons (E1 vertex omitted for the moment),

$$\sum_c \langle c|\mathcal{H}^e_{2\nu}|c\rangle \left\langle n,c\left|\frac{\alpha}{r_{12}}\right|n',c\right\rangle, \quad \sum_c \left\langle n,c\left|\frac{\alpha}{r_{12}}\right|n',c\right\rangle \langle c|\mathcal{H}^e_{2\nu}|c\rangle, \tag{8}$$

where r_{12} is the distance between two electrons. The quantum number of a single electron wave function, c, refers to one of the core electrons, while n, n' (which may or may not be the same) refers to the valence electrons.

In performing spatial integration of the neutrino emission vertex $\mathcal{H}^e_{2\nu}$, one essentially obtains the integrated electron number density of the core, since the wave vectors of plane neutrino wave functions hardly change within a single atom due to the much larger wavelength of emitted neutrinos. Hence, $\langle c|\mathcal{H}^e_{2\nu}|c\rangle =$ the weak coupling constants $\times$ two plane wave functions of neutrino pair at a target site. The remaining part is the Coulomb integral and its exchange integral between valence and core electrons,

$$\left\langle n,c\left|\frac{\alpha}{r_{12}}\right|n',c\right\rangle = \int d^3r_1 d^3r_2 \psi^*_n(\vec{r}_1)\psi^*_c(\vec{r}_2)\frac{\alpha}{|\vec{r}_1-\vec{r}_2|} \times \psi_{n'}(\vec{r}_1)\psi_c(\vec{r}_2) + (\text{exchange Coulomb integral}). \tag{9}$$

The exchange Coulomb integral turns out to be numerically much smaller, hence it is neglected. We shall use the Thomas-Fermi model [11] for an estimate of this quantity in heavy atoms. In the Appendix we give a basic explanation of the Thomas-Fermi model and how to compute the Coulomb integral in the model. The result for the Coulomb integral is summarized as

$$J_c \equiv \sum_c \left\langle n,c\left|\frac{\alpha}{r_{12}}\right|n',c\right\rangle = \frac{2^{10/3}}{(3\pi)^{2/3}} Z^{4/3}\frac{1}{2}\alpha^2 m_e \mathcal{J}_c, \tag{10}$$

$$\mathcal{J}_c \sim 0.23, \qquad J_c^2 \sim 50 Z^{8/3}\ \text{eV}^2. \tag{11}$$

In the Thomas-Fermi model dependence on the valence principal quantum numbers, n, n', is weak and we shall ignore it.

We next consider Coulomb-assisted neutrino pair emission from the nucleus, which turns out larger than that from core electrons. [The cancellation without Coulomb interaction works in this case too, in much the same way as in Eq. (7).] The relevant Z-exchange interaction arises from zeroth components of the quark current (4), which is conveniently written in terms of proton and neutron number densities,

$$\mathcal{H}^q_{2\nu} \sim \frac{G_F}{\sqrt{2}}\sum_i \nu_i^\dagger(1-\gamma_5)\nu_i j^0_q, \tag{12}$$

$$j^0_q = -\frac{1}{2}j^0_n + \frac{1}{2}(1-4\sin^2\theta_W)j^0_p, \tag{13}$$

where j^0_n, j^0_p are neutron and proton number densities. Coulomb-assisted pair emission for valence electron transition, $|n\rangle \to |n'\rangle$, contains

$$Q_w \sum_i \nu_i^\dagger \nu_i \left\langle n'\left|\frac{Z\alpha}{r}\right|n\right\rangle, \qquad Q_w = N - 0.044Z, \tag{14}$$

where N, Z is the neutron and the proton number of nucleus. The nucleus is assumed to be a point charge.

The Thomas-Fermi model gives an estimate of the Coulomb integral of this type. Its Z dependence is given by

$$J_N \equiv \left\langle n'\left|\frac{Z\alpha}{r}\right|n\right\rangle \sim \frac{2^{7/3}}{(3\pi)^{2/3}} Z^{4/3}\alpha^2 m_e \mathcal{J}_N, \quad \mathcal{J}_N = \int_0^\infty dx \frac{\chi(x)^{3/2}}{x^{1/2}}. \tag{15}$$

Numerically, we find that

$$\mathcal{J}_N \sim 1.6, \qquad (Q_w J_N)^2 \sim 2.5\times 10^3 Q_w^2 Z^{8/3}\ \text{eV}^2. \tag{16}$$

The ratio of two Coulomb integrals—the one from the nucleus to the one from core electrons—is of order $50Q_w^2$, thus the pair emission from nucleus dominates the process. RENP of some atomic processes, however, has no contribution of pair emission from the nucleus, and the pair emission from core electrons may become dominant. The enhancement factor of rates from nuclear monopole pair emission is roughly $(Q_w J_N)^2$ divided by squared energy spacing of atomic process.

The Thomas-Fermi model overestimates these Coulomb integrals compared with more precise calculations, since electrons are distributed more towards the center. We improved the model following [12] such that the potential is given by a sum of the inner core part of total charge $(Z-1)e$ provided by the Thomas-Fermi model and the shielded nuclear Coulomb potential of $-\alpha/r$. The nonrelativistic Schrödinger equation was then solved with this potential for a valence electron. This method gives a value for Ce J_N smaller by a factor ~2.5 than the Thomas-Fermi result. Nevertheless, we shall use the Thomas-Fermi estimate for Coulomb integrals in the rest of this work, for simplicity.

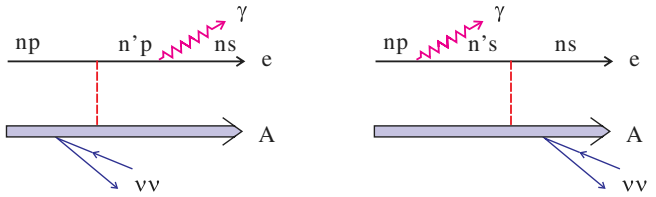

FIG. 1 (color online). First RENP diagrams for alkali atoms. Red dashed line is for Coulomb interaction between valence electron and nucleus.

The nuclear monopole contribution is insensitive to the elements of neutrino mixing matrix U_{ei}, since its contribution does not involve W-exchange interaction.

III. SPECTRUM RATE OF RENP

The Coulomb-assisted neutrino pair emission from nucleus or core electrons may be combined with E1 (electric dipole) transition from valence electrons. This is expected to give the largest RENP rate. We shall illustrate the calculation of Coulomb-assisted radiative emission of neutrino pair from the nucleus, taking alkali atoms of one valence electron.

With the Coulomb assistance, there are six types of diagrams equally contributing in absolute magnitudes, as shown in Figs. 1–3. There is a partial cancellations among six contributions: Contributions from the rightmost diagram of Fig. 1 and the two diagrams of Fig. 3 give a sum of the form

$$\begin{aligned} & Q_w\langle n's|\vec{d}\cdot\vec{E}|np\rangle\langle n's|V_C|ns\rangle \\ & \times\left(-\frac{1}{(\epsilon_{n's}-\epsilon_{np}+\omega)(\epsilon_{np}-\epsilon_{ns}-\omega)}\right. \\ & +\frac{1}{(\epsilon_{n's}-\epsilon_{ns})(\epsilon_{np}-\epsilon_{ns}-\omega)} \\ & \left.+\frac{1}{(\epsilon_{n's}-\epsilon_{ns})(\epsilon_{n's}-\epsilon_{np}+\omega)}\right), \end{aligned} \tag{17}$$

which vanishes exactly. The contributions of the rest are $\propto Q_w\langle ns|\vec{d}\cdot\vec{E}|n'p\rangle\langle n'p|V_C|np\rangle$, as given below in $F(\omega)$ of Eq. (19).

The RENP spectrum formula for alkali atomic transition $|n'p\rangle \to |ns\rangle+\gamma+\nu\nu, n'=n+1$ is given by

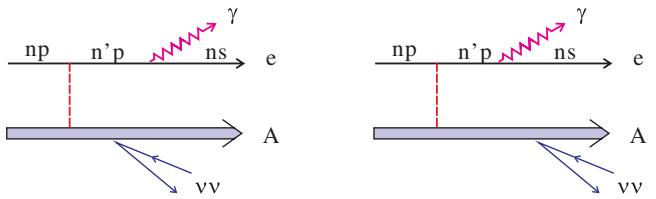

FIG. 2 (color online). Second RENP diagrams for alkali atoms.

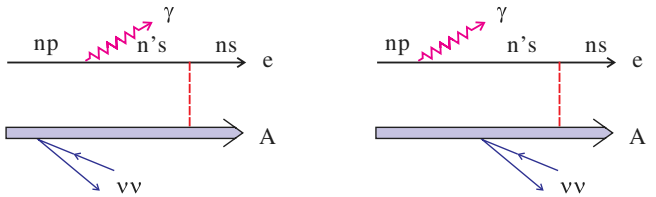

FIG. 3 (color online). Third RENP diagrams for alkali atoms.

$$\Gamma_{\gamma 2\nu}(\omega;t)=\Gamma_0 F^2(\omega)I(\omega)\eta_\omega(t), \qquad \Gamma_0=\frac{3}{4}G_F^2 n^3 V\epsilon_{\rm eg}, \tag{18}$$

$$\begin{aligned} F(\omega) &= \frac{Q_w J_N(\epsilon(n'p)-\epsilon(ns))}{\epsilon(n'p)-\epsilon(np)}\frac{1}{\sqrt{3\pi}} \\ &\quad\times\frac{d_{n'pns}}{(\epsilon(n'p)-\epsilon(np)+\omega)(\epsilon(np)-\epsilon(ns)-\omega)}, \\ d_{ab} &= \sqrt{3\pi\frac{\gamma_{ab}}{(\epsilon_a-\epsilon_b)^3}}, \end{aligned} \tag{19}$$

$$I(\omega)=\sum_i \Delta_i(\omega)I_i(\omega)\theta(\omega_{ii}-\omega), \qquad \omega_{ii}=\frac{\epsilon_{\rm eg}}{2}-\frac{2m_i^2}{\epsilon_{\rm eg}}, \tag{20}$$

$$\begin{aligned} I_i(\omega) &= \frac{\omega^2}{3}+\frac{2m_i^2\omega^2}{3\epsilon_{\rm eg}(\epsilon_{\rm eg}-2\omega)}+m_i^2(1+\delta_M), \\ \Delta_i(\omega) &= \left(1-\frac{4m_i^2}{\epsilon_{\rm eg}(\epsilon_{\rm eg}-2\omega)}\right)^{1/2}, \end{aligned} \tag{21}$$

with $\delta_M=1$ for the Majorana case and 0 for the Dirac case. The relation between transition dipole d_{ab} and transition rate γ_{ab} (A coefficient) has been used.

The photon energy spectrum from RENP is continuous below the threshold, slightly below the half of the energy difference of initial and final states, $\epsilon_{\rm eg}/2-2m_0^2/\epsilon_{\rm eg}$ with m_0 the smallest neutrino mass, hence is separated from the familiar D1 line of alkali atoms at $\epsilon_{\rm eg}$. The spontaneous (and not macrocoherent) emission spectrum of two-photon decay $|e\rangle\to|g\rangle+\gamma+\gamma$ is continuous starting from $\epsilon_{\rm eg}/2$, but has negligible rates.

The overall rate scale is given by Γ_0, which has the dimension of mass, or s^{-1}, in our natural unit of $\hbar=c=1$. Numerically, this value is

$$\Gamma_0\sim 54\ \text{m Hz}\frac{\epsilon_{\rm eg}}{\text{eV}}\left(\frac{n}{10^{21}\ \text{cm}^{-3}}\right)^3\frac{V}{10^2\ \text{cm}^3}\left(\frac{100\ \text{MHz}}{\text{eV}^3}\right)^{-1}. \tag{22}$$

As a reference parameter set, we took a target number density $n=10^{21}\ \text{cm}^{-3}$, a target volume $V=10^2\ \text{cm}^3$, A coefficients, γ_{ab}, in 100 MHz unit, and an available energy $\epsilon_{\rm eg}=1$ eV, along with all energies in the eV unit. The rate

dependence on these parameters is as explicitly indicated in this equation.

The extra factor n of the number density in the overall rate Γ_0 arises, since we replaced the field strength E^2 by its maximally stored energy density $\epsilon_{eg}n$ times the field storage fraction $\eta_\omega(t)$. The factor $\epsilon_{eg}n$ is equal to the atomic energy density stored in the upper level $|e\rangle$. The large factor n may be partially compensated by a small value of $\eta_\omega(t)$, and it is not clear that $\Gamma_0 \propto n^3$ automatically follows. But in accordance with the general idea of the macrocoherence the enhancement larger than n^2V is guaranteed in all cases. In any event the dependence $\propto n^3$ is a dynamical question which is resolved by more systematic simulations.

The spectral shape given by this formula is substantially different from the case of valence RENP in the preceding works of the spin current [5], in particular in the low-energy limit $\omega \to 0$. The reason for this is the presence of the nuclear monopole current in the neutrino emission vertex, which is different from the spin current in the valence RENP. The calculation leading to the spectral rate $I(\omega)$ is sketched in the Appendix.

The factor $\eta_\omega(t)$ is the extractable fraction of field intensity $\epsilon_{eg}n$ stored in the initial upper level $|e\rangle$. The storage and development of target polarization is induced by two trigger laser irradiation of $\omega_1 + \omega_2 = \epsilon(n'p) - \epsilon(ns), \omega_1 < \omega_2$. The storage is due to a second-order QED process, for instance M1 × E1 type of two-photon paired superradiance via virtual intermediate state $n'p_{1/2} \to n'p_{3/2} \to ns_{1/2}$ in alkali atoms. The calculation of $\eta_\omega(t)$ requires numerical solution of the master equation for developing fields and target polarization given in [5,6]. Usually, $\eta_\omega(t)$ is much less than unity, and depends on experimental conditions. In the present work we use a conservative value of $\eta_\omega(t)$ in the range 10^{-6} [13]. The macrocoherent development of field at frequency ω and macroscopic polarization between $n'p$ and ns up to a time range of several to ten nanoseconds is a prerequisite for experimental success of RENP. The macrocoherence is expected to decay after the phase relaxation time T_2.

We shall present the RENP spectrum rates for Cs and Xe, although the enhancement due to the monopole current is universal and may be applied to other target atoms as well. We shall first comment on how experiments may be performed. Typical RENP experiments use several lasers for trigger and excitation. For instance, two continuous wave (CW) lasers of different frequencies, $\omega_i, \omega_1 + \omega_2 = \epsilon_{eg}$ with ϵ_{eg} the energy difference between the initial $|e\rangle$ state and the final $|g\rangle$ state, are used as triggers in counterpropagating directions (taken along z axis), while two excitation lasers of Raman type of frequencies, ω_p, ω_s with $\omega_p - \omega_s = \epsilon_{eg}$, are irradiated in pulses. Measured variables at the time of excitation pulse irradiation are the number of events at each trigger frequency ω_1. By repeating measurements at different trigger frequency combinations, one obtains the photon energy spectrum at different frequencies $\omega = \omega_1 (< \omega_2)$ accompanying the neutrino pair. The single photon process, even if it can exist, is distinguished from RENP in the difference of energy spectrum: The RENP photon spectrum is continuous and starts slightly below half of the level difference by an amount of $2m_0^2/\epsilon_{eg}$ of the smallest neutrino mass m_0, while the macrocoherent single photon decay is monochromatic at the level difference.

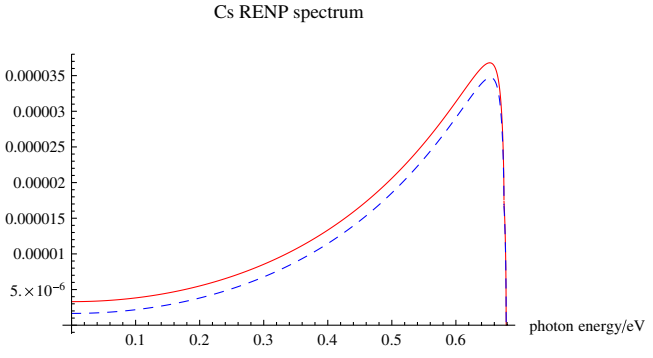

FIG. 4 (color online). Cs RENP spectrum from deexcitation of energy level at $6P_{1/2}(1.3859\ \text{eV})$, assuming the smallest neutrino mass of 0.1 eV in the normal hierarchical (NH) mass pattern, the Majorana case in solid red and the Dirac case in dashed blue, taking other masses and mixing angles consistent with neutrino oscillation experiments. The actual Cs RENP rate is obtained by multiplying $1.5 \times 10^5 (n/10^{21}\ \text{cm}^{-3})^3 \times (V/10^2\ \text{cm}^3)(\eta_\omega(t)/10^{-6})$ Hz.

In Figs. 4 and 5 we plot the spectral shape for ^{133}Cs. Cs data used are states $|e\rangle = 6P_{1/2}(1.3859\,\text{eV}), |g\rangle = 6S_{1/2}(0)$ and A coefficient $7.93 \times 10^5\ \text{s}^{-1}$ for $7P_{1/2}(2.6986) \to 6S_{1/2}$, taken from NIST [14]. For the smallest neutrino mass as large as 0.1 eV, as in this example, the Majorana vs Dirac distinction is possible by Cs RENP, but for smaller mass values it becomes difficult, requiring a large statistics data of RENP. The situation for MD distinction is improved for smaller atomic spacings [15].

As another example we take Xe atomic deexcitation from $6s^3P_1$ transition. This is an electron-hole system

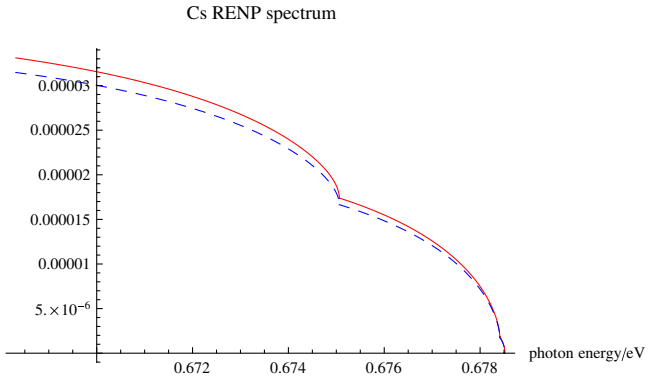

FIG. 5 (color online). Threshold region corresponding to Fig. 4.

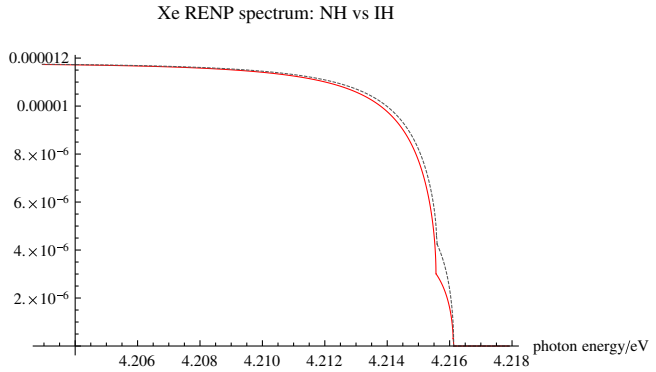

FIG. 6 (color online). Threshold region of Xe spectral shape for Dirac and Majorana RENP. The actual rate should be multiplied by $\sim 4 \times 10^3$ Hz for Xe gas density of 7×10^{19} cm^{-3}, volume 10^2 cm^3, and $\eta_\omega = 10^{-6}$. The case of Majorana NH of the smallest mass 0.1 eV is depicted in solid red and Majorana IH case of the same mass is depicted in dotted black. Majorana and Dirac cases are degenerate with this resolution.

consisting of a valence electron of 6s,7s,6p and a hole of 5p, its quantum number being much like a two-valence electron system. We shall use a different scheme from that considered in [5] to utilize the nuclear monopole contribution. Data used are energy levels of $6s^3P_1(8.437\ \text{eV})$ for the initial state and $7s^3P_1(10.593\ \text{eV})$, and its A coefficient, $\gamma_{7s5p} = 8.51 \times 10^7\ \text{s}^{-1}$. The RENP rate of ^{131}Xe from nuclear pair emission is given by

$$\Gamma_{\gamma 2\nu}(\omega; t) = \Gamma_0 F_X^2(\omega) I(\omega) \eta_\omega(t),$$
$$F_X(\omega) = \frac{Q_w J_N(\epsilon_{7s} - \epsilon_{6s})}{\epsilon_{7s} - \epsilon_{5p}} \frac{1}{\sqrt{3\pi}} \times \frac{d_{7s5p}}{(\epsilon_{7s} - \epsilon_{6s} + \omega)(\epsilon_{6s} - \epsilon_{5p} - \omega)}. \quad (23)$$

Abbreviated notations are used, paying attention to single electron transitions; for instance, $7s$ here means the atomic state $5p^5 7s$ and $5p$ is an orbital in the closed shell $5p^6$ with $\epsilon_{5p} = 0$ by definition of the energy origin.

Its spectral shape is given in Fig. 6, which shows that neutrino mass differences of this size and different hierarchical mass patterns can be differentiated. MD distinction is impossible with assumed neutrino masses. Although the RENP rate is much smaller due to the assumed atom density appropriate for a gas target, the gas target has a number of merits compared with solid targets, such as a larger phase relaxation time T_2.

IV. SUMMARY

We have presented a new enhancement mechanism of RENP due to the monopole vertex of neutrino pair emission from inner core electrons and nucleus in heavy atoms. The enhancement factor for RENP rates is very large, depending on the atomic number $\propto Z^{8/3}$ for pair emission from core electrons and $\propto Q_w^2 Z^{8/3}$ for pair emission from the nucleus, where $Q_w \sim N - 0.044Z$ is the electroweak neutral charge of the nucleus. Both rates and spectral shapes of emitted photon energy have been calculated and examples of Cs and Xe RENP have been provided. The new mechanism of monopole current opens a variety of possibilities in the selection of ideal RENP targets.

ACKNOWLEDGMENTS

We appreciate M. Tanaka for a discussion. This research was partially supported by Grant-in-Aid for Scientific Research on Innovative Areas "Extreme quantum world opened up by atoms" (Grant. No. 21104002) from the Ministry of Education, Culture, Sports, Science, and Technology.

APPENDIX A: COULOMB INTEGRAL IN THE THOMAS-FERMI MODEL

In the Thomas-Fermi model [11] one assumes the degenerate Fermi gas of electrons at each point of the atom, and relates the Fermi momentum to the number density. The kinetic energy at the Fermi momentum is balanced against the potential energy exerted to the electron. In other words, the pressure gradient of degenerate gas is balanced against the electrostatic potential. This gives a relation of the electron number density $n_e(r)$ to the potential $\varphi(r)$.

$$\frac{(3\pi^2 n_e(r))^{2/3}}{2m_e} - e\varphi(r) = 0. \quad (A1)$$

The spherical symmetry is assumed.

The second important equation is the Poisson equation, relating the electron number density to the potential. Combined with the density-potential relation above, one arrives at a self-consistent equation for the potential

$$\frac{1}{r}\frac{d^2}{dr^2}(r\varphi) = \frac{e}{3\pi^2}(2m_e e\varphi)^{3/2}. \quad (A2)$$

It is convenient to introduce dimensionless units of

$$\chi = \frac{4\pi}{Ze} r\varphi, \qquad r = bx, \quad (A3)$$

$$b = \frac{(3\pi)^{2/3}}{2^{7/3}} \frac{Z^{-1/3}}{\alpha m_e} \sim 0.8853 Z^{-1/3} a_B. \quad (A4)$$

The Thomas-Fermi equation is written for $\chi(x)$,

$$x^{1/2} \frac{d^2\chi}{d^2 x} = \chi^{3/2}. \quad (A5)$$

The asymptotic behavior with $x \to \infty$ is worked out, to give $\chi(x) \to 144/x^3$. The boundary condition at the origin is set from the physical setup, the nuclear charge, which dictates $\chi(x) \to 1$ as $x \to 0$, along with $\chi'(0) = 0$. The problem thus becomes an eigenvalue problem. The eigenfunction satisfies $\chi(x) = 1 - c_1 x + \cdots, c_1 \sim 1.588$ as $x \to 0$ [11]. The electron number density is given by

$$n_e = \frac{32}{9\pi^3} Z^2 (\alpha m_e)^3 \left(\frac{\chi}{x}\right)^{3/2}. \tag{A6}$$

The Coulomb interaction between a valence electron and all core electrons in the closed shell is given by

$$\int d^3 r_1 d^3 r_2 |\psi_n(\vec{r}_1)|^2 n_e(\vec{r}_2) \frac{\alpha}{|\vec{r}_1 - \vec{r}_2|} \equiv J_C. \tag{A7}$$

We may assume that dependence of this quantity on the quantum number of the valence electron n is weak, and define the Coulomb integral as αJ. This quantity is given in dimensionless units

$$J_C = \frac{(4\pi)^2}{(6\pi^4)^{2/3}} Z^{4/3} \frac{1}{2} \alpha^2 m_e \mathcal{J} \sim 31 \text{ eV} Z^{4/3} \mathcal{J}, \tag{A8}$$

$$\mathcal{J} = \int_0^\infty dx_1 x_1^{-1/2} (\chi(x_1))^{3/2} \int_0^{x_1} dx_2 x_2^{1/2} (\chi(x_2))^{3/2}. \tag{A9}$$

A value of $\mathcal{J} \sim 0.23$ is obtained by numerically solving the Thomas-Fermi equation and by integrating the results, to give

$$(J_C)^2 \sim 50 Z^{8/3} \text{ eV}^2. \tag{A10}$$

Another important integral used in the text is the Coulomb integral between the valence electron and the nucleus, which is

$$Z\alpha \int d^3 r_1 d^3 r_2 \frac{|\psi_N(\vec{r}_2)|^2 n_e(\vec{r}_1)}{|\vec{r}_1 - \vec{r}_2|} \sim \alpha \int d^3 r \frac{n_e(r)}{r}, \tag{A11}$$

in the small nucleus limit. The estimate of this quantity in the Thomas-Fermi model is

$$\frac{2^{7/3}}{(3\pi)^{2/3}} Z^{4/3} \alpha^2 m_e \int_0^\infty dx \frac{\chi(x)^{3/2}}{x^{1/2}} \sim 31 \text{ eV} Z^{4/3}. \tag{A12}$$

APPENDIX B: PHASE SPACE INTEGRAL OVER NEUTRINO MOMENTA

We start from the two-neutrino emission vertex (5), its square to be multiplied by E1 photon emission factor $(\vec{d} \cdot \vec{E})^2$ from the valence electron and by the Coulomb factor F of Eq. (19) for rates. Here we concentrate on summation over helicities and momenta of two emitted neutrinos.

Using the helicity summation formula of [4],

$$\sum_{h_i} |j_\nu \cdot j^{e,q} A|^2 = \frac{1}{2}\left(1 + \frac{\vec{p}_1 \cdot \vec{p}_2}{E_1 E_2} + \delta_M \frac{m_1 m_2}{E_1 E_2}\right) \times j_0^{e,q} (j_0^{e,q})^\dagger |A|^2 + \cdots, \tag{B1}$$

where $j_0^{e,q}$ is the zeroth component electron/quark current, and $(E_i, \vec{p}_i)$ are neutrino four-momenta. The function A refers to all the rest of amplitudes including QED vertex, energy denominators, and all coupling constants. In previous works on valence RENP, the three-vector part $\propto \vec{j}_e$ of electron current (spin current),

$$\sum_{h_i} |j_\nu \cdot j^e A|^2 = \frac{1}{2}\left(1 - \frac{\vec{p}_1 \cdot \vec{p}_2}{E_1 E_2} - \delta_M \frac{m_1 m_2}{E_1 E_2}\right) \vec{j}_e \cdot \vec{j}_e^\dagger |A|^2 + \frac{\vec{p}_1 \cdot \vec{j}^e \vec{p}_2 \cdot \vec{j} |A|^2}{E_1 E_2} + \cdots, \tag{B2}$$

has been relevant. The difference of the sign $\pm \frac{\vec{p}_1 \cdot \vec{p}_2}{E_1 E_2}$ appears in the suppressed region of the spectrum: For the monopole current (B1) the low-energy limit $\omega \sim 0$ neutrino momenta are nearly balanced, $\vec{p}_1 \sim -\vec{p}_2$, and there is more suppression in the low-energy limit for the monopole case. In Eqs. (B1) and (B2) we neglected time reversal odd terms.

In the phase space integral of neutrino momenta,

$$\int \frac{d^3 p_1 d^3 p_2}{(2\pi)^2} \delta(E_1 + E_2 + \omega - \epsilon_{\text{eg}}) \delta(\vec{p}_1 + \vec{p}_2 + \vec{k})(\cdots), \tag{B3}$$

one of the momentum integration is used to eliminate the delta function of the momentum conservation. The resulting energy conservation is used to fix the relative angle factor $\cos\theta$ between the photon and the remaining neutrino momenta, $\vec{p}_1 \cdot \vec{k} = p_1 \omega \cos\theta$. Noting the Jacobian factor $E_2/p\omega$ from the variable change to the cosine angle, one obtains a one-dimensional integral over the neutrino energy E_1,

$$I_{ij}(\omega) \frac{\Delta_{ij}(\omega)}{2\pi} \equiv \frac{1}{2\pi\omega} \int_{E_-}^{E_+} dE_1 E_1 E_2 \frac{1}{2} \times \left(1 + \frac{\vec{p}_1 \cdot \vec{p}_2}{E_1 E_2} + \delta_M \frac{m_1 m_2}{E_1 E_2}\right), \quad E_2 = \epsilon_{\text{eg}} - \omega - E_1. \tag{B4}$$

The angle factor constraint $|\cos\theta| \leq 1$ places a constraint on the range of neutrino energy integration,

$$E_{\pm} = \frac{1}{2}\left((\epsilon_{\rm eg}-\omega)\left(1+\frac{m_i^2-m_j^2}{\epsilon_{\rm eg}(\epsilon_{\rm eg}-2\omega)}\right) \pm \omega\Delta_{ij}(\omega)\right), \tag{B5}$$

$$\Delta_{ij}(\omega) = \left\{\left(1-\frac{(m_i+m_j)^2}{\epsilon_{\rm eg}(\epsilon_{\rm eg}-2\omega)}\right)\left(1-\frac{(m_i-m_j)^2}{\epsilon_{\rm eg}(\epsilon_{\rm eg}-2\omega)}\right)\right\}^{1/2}. \tag{B6}$$

The integrand is a quadratic function of neutrino energy [15], and it is easily integrated to give

$$I_{ij}(\omega) = \frac{\omega^2}{3}+\frac{1}{2}(m_i^2+m_j^2)+\frac{1}{3}\frac{\omega^2(m_i^2+m_j^2)}{\epsilon_{\rm eg}(\epsilon_{\rm eg}-2\omega)} - \frac{3}{4}\frac{(\epsilon_{\rm eg}-\omega)^2}{\epsilon_{\rm eg}^2(\epsilon_{\rm eg}-2\omega)^2}(m_i^2-m_j^2)^2+\delta_M m_i m_j. \tag{B7}$$

The result, $I_i(\omega) = I_{ii}(\omega)$, is needed in Eq. (21) and in other places of the text.

[1] G. L. Fogli, E. Lisi, A. Marrone, D. Montanino, A. Palazzo, and A. M. Rotunno, Phys. Rev. D **86**, 013012 (2012); M. C. Gonzalez-Garcia, M. Maltoni, J. Salvado, T. Schwetz, J. High Energy Phys. 12 (2012) 123; D. V. Forero, M. Toacutertola, and J. W. F. Valle, Phys. Rev. D **86**, 073012 (2012).

[2] G. Drexlin, V. Hannen, S. Mertens, and C. Weinheimer, Adv. High Energy Phys. (2013) 293986.

[3] A. Gando *et al.*, Phys. Rev. Lett. **110**, 062502 (2013); KamLAND-Zen Collaboration, Phys. Rev. C **85**, 045504 (2012); M. Auger *et al.*, Phys. Rev. Lett. **109**, 032505 (2012).

[4] M. Yoshimura, Phys. Rev. D **75**, 113007 (2007).

[5] A. Fukumi *et al.*, Prog. Theor. Exp. Phys. (2012) 04D002, and references therein.

[6] M. Yoshimura, N. Sasao, and M. Tanaka, Phys. Rev. A **86**, 013812 (2012).

[7] M. A. Bouchiat and C. Bouchiat, J. Phys. (Paris) **35**, 899 (1974).

[8] M. A. Bouchiat, J. Guena, L. Pottier, and L. Hunter, Phys. Lett. **134B**, 463 (1984), and references therein.

[9] P. S. Drell and E. D. Commins, Phys. Rev. A **32**, 2196 (1985), and references therein.

[10] M. C. Noecker, B. P. Materson, and C. E. Wieman, Phys. Rev. Lett. **61**, 310 (1988), and references therein.

[11] B. H. Bransden and C. J. Joachain, *Physics of Atoms and Molecules* (Prentice Hall, Englewood Cliffs, NJ, 2003), 2nd ed., Chap. 8.3.

[12] D. Neuffer and E. D. Commins, Phys. Rev. A **16**, 844 (1977).

[13] In [5] a result for numerical simulation of $\eta_\omega(t)$ is presented for pH_2 molecule target (strong source of paired superradiance (PSR) of E1 × E1 transition, and see Fig. 14 of this reference for time dependence). Its time dependence is complicated: a fast rise in $O(2$ ns), then a plateau region of magnitude $O(10^{-2}-10^{-3})$ of duration of several nanoseconds, and finally a gradual decrease ending around 10^{-6} at ~ 12 ns (end time of calculation). For RENP rate calculations, numerical simulations based on the master equation given in [5] should be performed for weaker PSR process of specific targets considered, which is expected to give different time profiles and larger values of $\eta_\omega(t)$.

[14] National Institute of Standards and Technology (NIST) Atomic Spectra Database. http://www.nist.gov.

[15] D. N. Dinh, S. Petcov, N. Sasao, M. Tanaka, and M. Yoshimura, Phys. Lett. B **719**, 154 (2013).